

High resolution wind resource assessment over complex terrain: influence of 4D data assimilation in the WRF-LES wind model

Pablo Cárdenas¹, Alex Flores^{1*}, Joaquín Mura¹

¹Federico Santa María Technical University, Department of Mechanical Engineering, Valparaíso, Chile

*Corresponding author email: alex.floresm@usm.cl

Abstract: To develop a reliable tool for accurate evaluations of the wind behavior over both flat and complex terrain, a novel methodology that assimilates field measurements at surface level for multiscale wind simulations was implemented and tested in the Weather Research and Forecasting model (WRF-ARW). The proposed method was applied to perform high resolution simulations, i.e. mesh sizes up to 2 m, of real case studies with nested domains and the introduction of a variational data assimilation (DA) technique of field observations, from databases registered for specific experiments over heterogeneous topography. In the inner domains, the atmospheric boundary layer (ABL) parameterization was executed with a 1.5 TKE turbulence scheme for large-eddy simulation (LES), employed to obtain detailed realizations of the anisotropic turbulence of the surface layer. Field data was introduced in the innermost domain through a 4D data assimilation system to correct the numerical deviations every 10 minutes in the first 6 hours of the simulation. Four experiments are presented, in two separate scenarios: (i) the Høvsøre case, at Denmark, to replicate a neutrally stratified wind flow over real flat terrain, in which the DA process was accomplished through a three layer single-point met-mast measurement located at the domain center and (ii) the Bolund case, at Denmark, to realize a neutrally stratified wind flow over steep complex terrain, where the DA was taken from 8 met-masts distributed in a neural network across the domain. Validation of this approach was made for each case by contrasting the modelling results with field observations from campaign databases and related literature. The outcomes show that it is possible to obtain more accurate predictions of surface wind flow, replicating the nonlinear turbulent phenomena at finescale and that employing data assimilation reduces the wind estimations and predictions over real topography by 10%. In presence of very steep terrain, the 4D assimilation technique needs further improvement due to the proximity of field measurements to the ground and strong terrain induced forcing, which impose a tough constraint on high resolution wind modelling.

Keywords: Wind resource assessment; multiscale wind modelling; data assimilation; large-eddy simulation; complex terrain.

1 Introduction

The growing demand for cleaner energy sources in power generation due to global warming and environmental issues makes it necessary to use new tools to support the investment decision-making in these projects. Specifically, if one speaks of wind energy, variables such as wind speed, direction and gradient must be predicted effectively and efficiently to respond to the electrical coordination or identify failures due to undesirable mechanical stresses in the turbines. Historically two ways has been taken to predict the wind behavior. The first is an statistical approach that uses data from several meteorological masts or other instrumentation located in a domain to extrapolate information to a time of interest. This approach present some weakness: (i) dependency of the instrumentation, (ii) the historical databases can't capture actual and local conditions of the atmosphere such as climate change, and (iii) the statistical values don't show the behavior of the continuous terrain but in some arbitrary points. Is because this that for more specific goals a second approach is used: the Numerical Weather Prediction (NWP). The NWP target is to find the future state of the meteorological variables by integration of the partial differential equations system that models the atmosphere behavior. One of the most relevant property of this system is the presence of multiples scales, i.e. the preponderant forces that governs the air dynamics vary depending of the space-temporal scale to analyze. Is convenient then to separate the spatial dependence associating a characteristic length to the domain of interest, in this way a global scale, synoptic scale, mesoscale and microscale can be defined. This scales multiplicity introduces a new challenge to overcome: the computational cost of solving a system of equations valid for the entire atmosphere. Consequence of this, a spectrum of numerical models have been created specifically for each spatial scale with their own equations, but

the initialization of a small-scale model requires the results of a larger one. With respect to global models, these have shown to be able to correctly simulate many aspects of the general circulation of the atmosphere ([Stocker et al. 2013](#)), however, for engineering interests, the focus is on the local behavior of the wind, specifically, how it moves within the planetary boundary layer (PBL) which is the part of the atmosphere we inhabit and that is outside the resolution of these models. The approach being used today for small-scale atmospheric simulation, i.e. solving the structures belonging to the PBL, is through the so-called dynamic downscaling, interpolating the results from a large-scale model to a small-scale model in order to function as a boundary condition and generate a forecast in a finer mesh. This method defines what is understood by multi-scale simulation and this type of simulation is still widely discussed by the scientific community ([Arnold et al. 2010](#)). The use of dynamic downscaling proved to be successful at least in the spectrum of global and synoptic scales. Numerical issues arise in the mesoscale due to terrain forcing and the relevance of local surface fluxes. The reduction to the microscale causes the increase in the relevance of turbulent stresses in the equations, requiring a much more precise handling. Due to the space-time numerical grid dimensions in large scale models, the turbulence associated with the interaction with the surface and the thermal effects are generally parameterized through a turbulent viscosity model. In scales close to the microscale, the models start natively to solve the turbulent structures generating a problem due to the double weighting of these structures as they are being solved on the one hand and parameterized on the other. This zone is known as the grey zone ([Wyngaard 2004](#)) and an incorrect configuration of the dynamic downscaling in this zone can cause non-physical results of the model. At the microscale it is possible to represent the turbulence according to known numerical models such as LES or RANS depending on the case. Atmospheric models such as WRF have been widely used in recent years to predict wind behavior at the mesoscale through multiscale simulations, but only a few studies have addressed this behavior at the microscale in real simulations. The researches that analyze the behavior of the LES to represent the PBL generally use ideal conditions (e.g. periodic boundary conditions, flat terrain, imposed pressure gradients) which allows the validation of the approach, but at the cost of losing the operativeness of working in a realistic scenarios. Simulating a real case implies the use of high resolution databases for terrain elevation and land use category. In this work, in order to obtain the best possible solution for a short-term wind forecast in PBL, the use of a 4D data assimilation system was also considered with measurements obtained in the surface proximity within the simulation time window.

Lastly, the philosophy of this work is to establish the foundations of a new method for assessing the wind resource without relying on ad hoc idealizations, but through fundamental physics and the correct implementation of state-of-the-art instrumentation. The results obtained will serve as a benchmark for future verification of new or experimental models that perform high-resolution simulations in real terrain.

2 Methodology

2.1 ARW-WRF Atmospheric Model and Large Eddy Simulation

The WRF model is a state-of-the-art numerical mesoscale model that represent the latest scientific and engineering developments in climate prediction. It is open source, flexible, portable and efficient so that it allows simulations on both notebooks and massively parallelized supercomputers ([Skamarock et al. 2008](#)). In this work, the 3.8.1 version was used. It solves the non-hydrostatic Euler equations for fully compressible flow through a finite difference scheme. Spatial discretization is carried out through a C-Arakawa horizontal grid and a ground-following vertical grid based on hydrostatic dry air pressure. Temporal integration is carried out with a 2nd order Runge-Kutta scheme and the pressure waves that arises due to the model compressibility are filtered from the mean field through a divergence filter and are resolved in a time sub-step (1/3 of the external mode) to ensure the stability of the model. Boundary and initial conditions are specified from the results of a global model. A constant pressure condition with a damping layer is used at the upper boundary and wall functions are used at the soil surface through the surface layer parametrization.

The physical phenomena that lies within the model's mesh resolution are parameterized through several advanced schemes provided by the WRF team. Radiation, phase-change, cloud formation, surface interaction, boundary layer transport and turbulence are all considered within the model and are included in the right side

of the equations as dependent terms. Regarding turbulence, for the mesoscale it is represented by a vertical eddy viscosity that is computed in the PBL parametrization subroutine, while the horizontal eddy viscosity is computed through a Smagorinsky closure (Smagorinsky 1963). On the microscale, the PBL parametrization is turned off and a LES 1.5TKE model is used (Deardorff 1980). The LES package in WRF (Yamaguchi and Feingold 2012), expresses the eddy viscosity as:

$$v_t = c_k \ell \sqrt{k}, \quad (1)$$

where c_k is the constant of the TKE model ($0.15 \sim 0.30$) and k is the sub-grid kinetic energy defined as:

$$k = \frac{1}{2} \tau_{nn}. \quad (2)$$

The characteristic length ℓ of the model is computed as:

$$\ell = \begin{cases} \min[(\Delta x \Delta y \Delta z)^{1/3}, 0.76 \sqrt{k}/N] & N^2 > 0 \\ (\Delta x \Delta y \Delta z)^{1/3} & N^2 \leq 0 \end{cases} \quad (3)$$

Where N is the Brunt-Väisälä frequency for humid air. The value of k in each domain cell is calculated based on the transport equation defined by Skamarock et al. (2008).

2.2 Data Assimilation Process

From the WRF model, three-dimensional arrays of resolved meteorological variables (background) are obtained for a given time. The data assimilation (DA) goal is to physically weight the field measurements (observations) with these results to obtain the best estimate of the state of the atmosphere (analysis). Theoretically, the DA tries to minimize the cost function $J(x)$ that weighs the errors coming from the background J_b and from observations J_o :

$$J(x) = J_b + J_o = \frac{1}{2}(x - x_b)^T B^{-1}(x - x_b) + \frac{1}{2}(Hx - y)^T R^{-1}(Hx - y) \quad (4)$$

Here B is the background variance or error matrix (from the model), R is the observation error matrix (from the instruments) and H is the observation operator that performs a 3D interpolation of the numerical grid values to the observation space. This equation is solved recursively using a Quasi-Newtonian minimization algorithm.

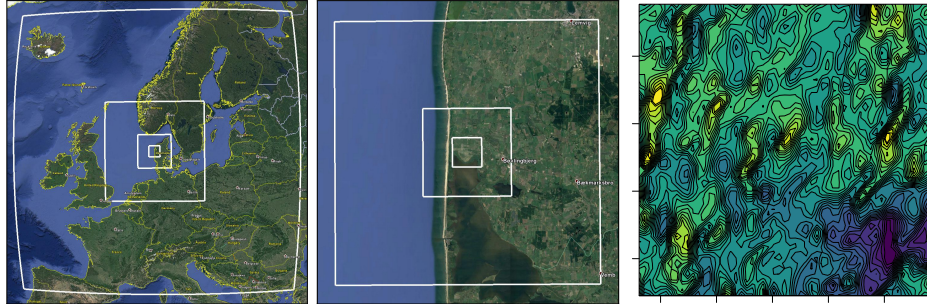


Figure 1: (Left-Center) Simulation domains for H1-H2. (Right) Resolved velocity contour at the innermost domain at UTC 15:00. $\Delta x = 25m$ in the innermost domain.

2.3 Case Study Settings

The goal of this study is to evaluate the behavior of the WRF mesoscale model in its LES mode when forced up to 3m mesh size while incorporating surface data assimilation within the PBL. Four experiments were developed for this purpose. The first two were carried out at Høvsøre (Peña et al. 2015; 2013; Floors et al. 2013) for the case without (H1) and with DA (H2). The last two correspond to simulations made in the Bolund Hill (Berg et al. 2011; Bechmann et al. 2009; 2011) for the case without (B1) and with DA (B2). The simulation's high resolution is achieved through the implementation of non-native WRF databases and downscaling The ASTER

database was used for the terrain height and Corine 2012 database (Pineda et al. 2004) was used for land use category. As for the downscaling, nested domains with feedback were used (7 for H-experiments and 8 for B-experiment). The subdomains were selected as to avoid the double weighting due to the turbulent grey zone (Wyngaard 2004). The standard 3:1 ratio was used in the meso and microscale and a 5:1 ratio (Green and Zhang 2015) for the domains where the shift to the microscale occurs (*terra incognita*). Initial and boundary condition of the coarser mesh is given by the operational analysis of the GFS global model with 0.5° of resolution. The boundary condition was mapped to the first domain border using a buffer zone of 5 elements of mesh and are updated every 6 hours. The configuration of the domains was subjected to a sensitivity analysis in order to adjust the best values to ensure: (i) the model stability, (ii) the convergence of results for the boundary layer and (iii) the lowest computation time. In this fashion, the number of elements for the mesh and the top boundary condition are established. The number of nodes in all the domains are set as $107 \times 107 \times 37$ for H-experiments and $107 \times 107 \times 41$ for B-experiment (except for the innermost domain which is $107 \times 92 \times 41$ due to the terrain database). For the vertical mesh, special care is taken to refine it so it is consistent with the application of the LES. In the first level there is an aspect ratio of $\Delta_x/\Delta_{z_1} = 2.35$ (see Figure 2) and this is progressively reduced in the higher levels. Lastly, the data needed to feed the data assimilation process comes from meteorological masts located within the innermost domain in each experiment. For the H-experiments there is one mast located at the center and for the B-experiments there are 8 masts distributed as shown in Figure 2. The frequency at which the background is corrected is set at 10 minutes and is performed during the first 6 hours of the simulation. The variables that were assimilated are wind speed and direction, and are assimilated at 10, 40, 60, 80 and 100 meters above the ground for H-experiments and 2, 5 and 9 meters for B-experiments.

For H-experiments, the performed simulations consists of a total of 14 hours, where the first 6 correspond to the spinup of the model and the time window where the data assimilation is applied. The date of the simulation were selected in such a way that it corresponds to a period with neutral atmospheric stability as declared by Peña et al. (2013) in its case 5, i.e. 08/09/2010 from 06:00 to 20:00, and the validation was done through comparison with values from that measurement campaign.

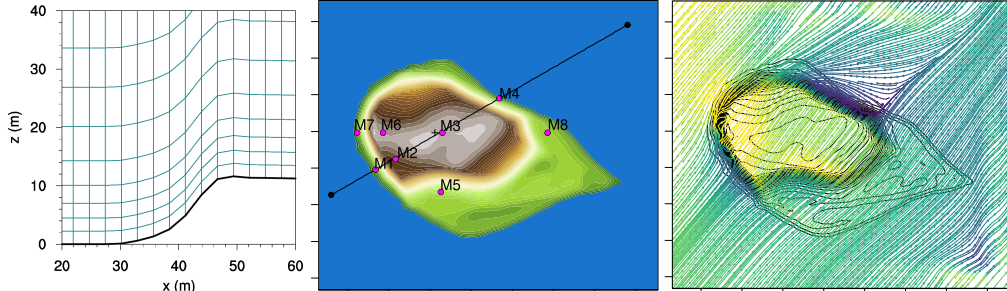


Figure 2: (Left) Detail the steep slope in M1-M4 cut. (Center) Control points locations for B1-2. (Right) Resolved streamlines in the first level of B1 at UTC 15:00. $\Delta x = 2.74\text{m}$ in the innermost domain.

The B-experiments consisted of 9 hours of simulation, with the first 6 hours being used for spinup and DA. The date was selected according to what was declared by Bechmann et al. (2009) for a day with the most neutral stratification possible, i.e. 29/12/2007 from 06:00 to 15:00. The validation was carried out by contrasting the values given for the blind comparison.

To evaluate the performance of the simulations in relation to the real data, RMSE and the MAE applied to the wind speed are used as metrics.

$$\text{MAE} = \frac{1}{n} \sum_{i=1}^n |V_m - V_o| \quad ; \quad \text{RMSE} = \sqrt{\frac{1}{n} \sum_{i=1}^n (V_m - V_o)^2} \quad (5)$$

Where V_o is the observed speed and V_m is the modelled speed. The evaluation these metrics was performed after the spinup time and each of the measured values is compared with the nearest simulated value, interpolated

to the corresponding height in the mast. The interpolation is made using a simple logarithmic law for the wind profile,

$$u(z) = u(z_r) \frac{\ln(z/z_0)}{\ln(z_r/z_0)} \quad (6)$$

Where z_0 is the corresponding roughness length for each case (Peña et al. 2013; Bechmann et al. 2011).

3 Remarkable Results and Conclusions

A simulation performance metric without the inclusion of DA can be seen in Figures 3 and 4 for experiments H1 and B1 respectively,

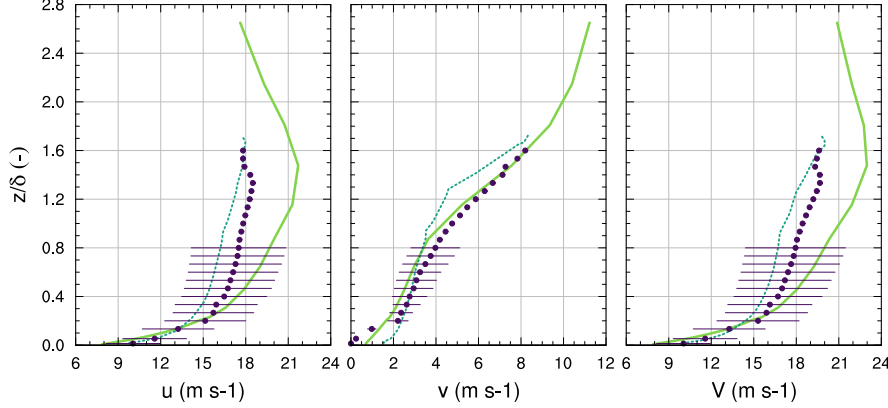


Figure 3: Comparison of the H1 speed results (continuous line) vs. the simulation of Peña et. al. in 2013 (dotted line) and measured values (points). The data correspond to time averages between 12:00 and 15:00.

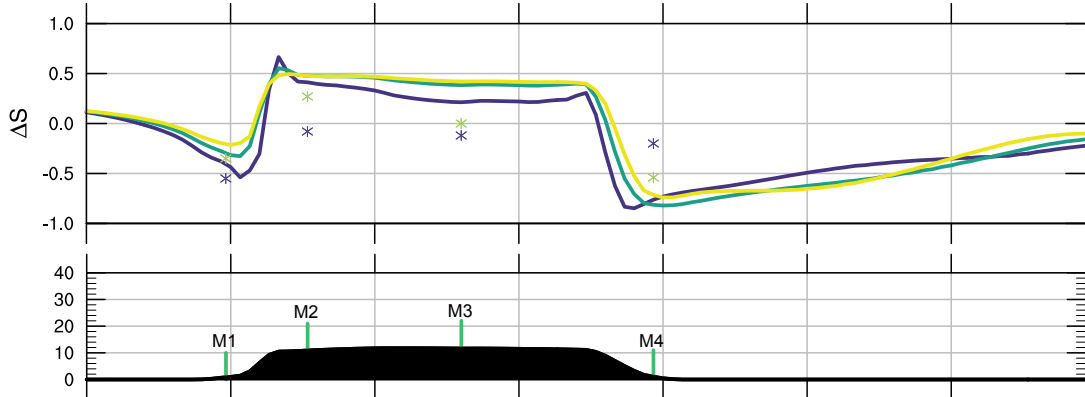


Figure 4: Comparison of B1 speedup results at 15:00 vs. blind comparison. Values for the first 3 levels (1.1m blue; 3.4m green; 5.6m yellow) in section M1-M4 are shown.

Here one can note that the high-resolution simulations met the expectations with respect to capturing: (i) the benchmark values for wind speed according to the validation cases and (ii) the qualitative behavior of the flow, both for flat terrain, as shown in Figure 1, where the structures of the LES can be seen, and for complex terrain (Figure 2) where the streamlines expose the downstream boundary layer separation from the hill.

Regarding the performance of the DA, the Figures 5 and 6 show the compared time series for a reference mast respectively. Note how in the first 6 hours of simulation (spinup) the data assimilation fixes the values to those measured.

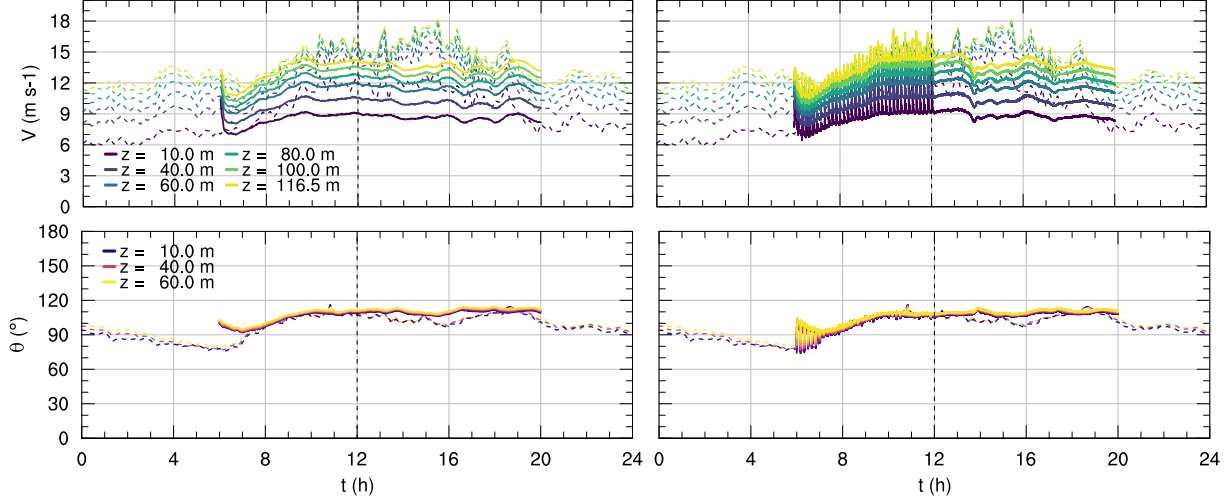


Figure 5: Time series for H1 vs. H2 at the met-mast. Simulation (solid line). Field data (dotted line)

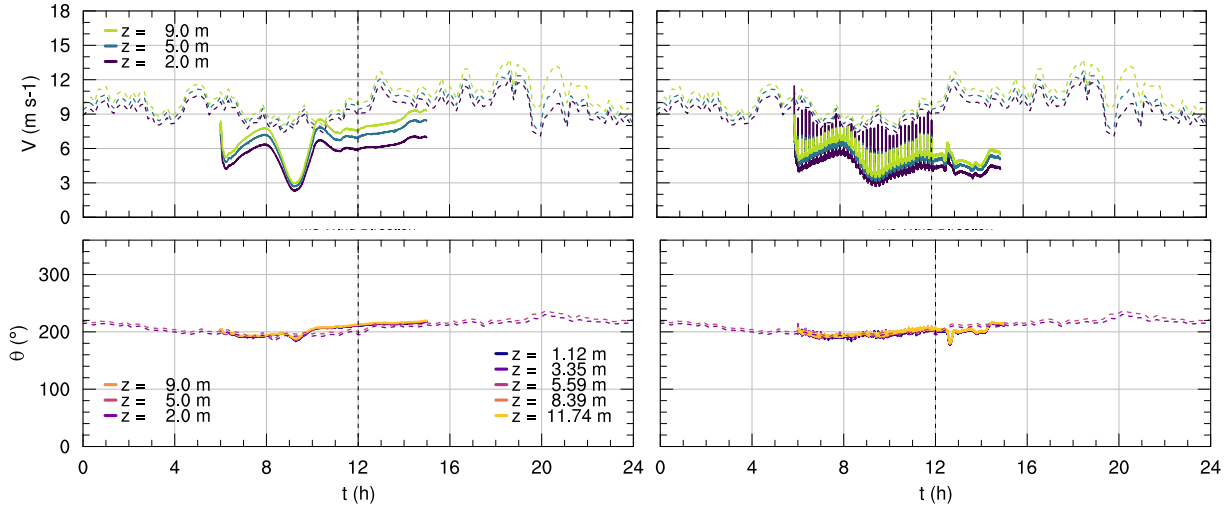


Figure 6: Time series for B1 vs. B2 at the M4 mast. Simulation (solid line). Field data (dotted line)

Wind direction is broadly well represented in both simulations. The speed on the contrary acts differently in the two cases. For the H-experiments, there is a momentum deficit at low levels, possibly due to an overdiffusion in the LES. On the other hand, the simulation fails to capture the acceleration generated between 14:00 and 15:00 hours, and even though the application of DA allows to correct part of the deficit, it is still unsatisfactory for operational use. For B-experiments, the speed deficit in the low levels still exists, but in addition, it can be seen that the addition of DA negatively affects the performance of the simulation.

Table 1: Velocity metric comparison for all experiments in (m s⁻¹)

	H1	H2	B1	B2
MAE	2.41	2.17	2.67	4.36
RMSE	2.80	2.56	2.95	4.90

The quantitative performance of the DA can be seen by using the defined metrics. Table 1 shows the summary for all cases. Here it can be seen that for the flat terrain case there is an improvement of about 10% in the wind estimation, but for the complex terrain case the solution gets worse by almost 60%.

To conclude, it is relevant to highlight the following points:

- It is possible to carry out microscale simulations through a mesoscale model that are satisfactory in both first order variables and wind behavior. The way to do this is by (i) using appropriate databases for terrain height and land use category and (ii) unifying the scales through an LES model. The simulated values for the H1 and B1 experiments show agreement with those presented in the literature using other types of methodologies.
- Even though data assimilation proved improvements for the flat terrain case, the non-linearity of the complex terrain did not allow the DA to permeate to an improvement in the prediction of the wind resource. In addition to this, it is necessary to carry out more field experiments in order to have access to a larger amount of data in more masts and in this way to experiment with different data assimilation schemes for the improvement of simulations. In this work, data was assimilated within the boundary layer, stressing the associated turbulence model. One way to relax this is to assimilate data both inside and outside the boundary layer and in greater numbers across the domain.

4 Acknowledgements

The authors wish to sincerely thanks the Chilean National Commission for Scientific and Technological Research (CONICYT) for funding this research through project FONDEF ID16I10105, the Federico Santa María Technical University for its support through project PI-LI-19-04 and the DTU Vindenergi for providing access to the data for the development of this research.

References

- Arnold D, Schicker I, Seibert P (2010) High-resolution atmospheric modelling in complex terrain for future climate simulations (HiRmod). Tech. rep., Institute of Meteorology (BOKU-Met), University of Natural Resources and Life Sciences
- Bechmann A, Berg J, Courtney M, Ejsging Jørgensen H, Mann J, Sørensen N (2009) The Bolund Experiment: Overview and Background. Danmarks Tekniske Universitet, Risø Nationallaboratoriet for Bæredygtig Energi, risø-R-1658(EN)
- Bechmann A, Sørensen NN, Berg J, Mann J, Réthoné PE (2011) The bolund experiment, part II: Blind comparison of microscale flow models. *Boundary-Layer Meteorology* 141(2):245–271
- Berg J, Mann J, Bechmann A, Courtney MS, Jørgensen HE (2011) The bolund experiment, part I: Flow over a steep, three-dimensional hill. *Boundary-Layer Meteorology* 141(2):219–243
- Deardorff JW (1980) Stratocumulus-capped mixed layers derived from a three-dimensional model. *Boundary-Layer Meteorology* 18(4):495–527
- Floors R, Vincent CL, Gryning SE, Peña A, Batchvarova E (2013) The wind profile in the coastal boundary layer: Wind lidar measurements and numerical modelling. *Boundary-layer meteorology* 147(3):469–491
- Green BW, Zhang F (2015) Numerical simulations of Hurricane Katrina (2005) in the turbulent gray zone. *Journal of Advances in Modeling Earth Systems* 7(1):142–161
- Peña A, Floors R, Gryning SE (2013) The Høvsøre tall wind-profile experiment: A description of wind profile observations in the atmospheric boundary layer. *Boundary-Layer Meteorology* 150(1):69–89
- Peña A, Floors R, Sathe A, Gryning SE, Wagner R, Courtney MS, Larsén XG, Hahmann AN, Hasager CB (2015) Ten years of boundary-layer and wind-power meteorology at Høvsøre, denmark. *Boundary-Layer Meteorology* 158(1):1–26

Pineda N, Jorba O, Jorge J, Baldasano JM (2004) Using NOAA AVHRR and SPOT VGT data to estimate surface parameters: application to a mesoscale meteorological model. International Journal of Remote Sensing 25(1):129–143

Skamarock W, Klemp J, Dudhia J, Gill D, Barker D, Wang W, Huang XY, Duda M (2008) A description of the advanced research WRF version 3

Smagorinsky J (1963) General circulation experiments with the primitive equations. Monthly Weather Review 91(3):99–164

Stocker TF, Qin D, Plattner GK, Tignor M, Allen SK, Boschung J, Nauels A, Xia Y, Bex V, Midgley PM, et al. (2013) Climate change 2013: The physical science basis

Wyngaard JC (2004) Toward numerical modeling in the “Terra Incognita”. Journal of the Atmospheric Sciences 61(14):1816–1826

Yamaguchi T, Feingold G (2012) Large-eddy simulation of cloudy boundary layer with the advanced research WRF model. Journal of Advances in Modeling Earth Systems 4(3)